Gupta *et al.*
Protection and Control of Modern Power Systems (2022) 7:33
https://doi.org/10.1186/s41601-022-00255-w

Protection and Control of Modern Power Systems

ORIGINAL RESEARCH Open Access

Design of a 2-DOF-PID controller using an improved sine–cosine algorithm for load frequency control of a three-area system with nonlinearities

Neelesh Kumar Gupta*, Manoj Kumar Kar and Arun Kumar Singh

Abstract

This paper proposes an improved sine–cosine algorithm (ISCA) based 2-DOF-PID controller for load frequency control. A three-area test system is built for study, while some physical constraints (nonlinearities) are considered for the investigation of a realistic power system. The proposed method is used as the parameter optimizer of the LFC controller in different scenarios. The 2-DOF-PID controllers are used because of their capability of fast disturbance rejection without significant increase of overshoot in set-point tracking. The 2-DOF-PID controllers' efficacy is observed by examining the responses with the outcomes obtained with PID and FOPID controllers. The simulation results with the suggested scheme are correlated with some of the existing algorithms, such as SCA, SSA, ALO, and PSO in three different scenarios, i.e., a disturbance in two areas, in three areas, and in the presence of physical constraints. In addition, the study is extended to a four-area power system. Statistical analysis is performed using the Wilcoxon Sign Rank Test (WSRT) on 20 independent runs. This confirms the supremacy of the proposed method.

Keywords: 2-DOF-PID, FOPID, Load frequency control, WSRT, Statistical analysis, Improved sine–cosine algorithm

1 Introduction

1.1 Literature survey

The pivotal aspiration of the modern power system is to provide a reliable power supply without any interruption. This can be achieved when equilibrium between demand and generation of power is maintained. Frequency is one of the vital parameters which indicates the balance between demand and supply or generation. As frequency and load are inversely proportional to each other, frequency increases when the load is less than the generation, while frequency reduces when the load on the system is more than the supply. Maintaining the frequency at its standard value is an essential task and can be achieved by a technique known as load frequency control (LFC) [1]. LFC has the significant responsibility to maintain the drift in frequency within the permissible limit. In addition, it also maintains the drift in tie-line power between multi-area systems to its permissible value. The mechanical input to the power generator is provided to have a balance between generation and demand of power and thereby, LFC controls the input to the generator according to the requirements. LFC basically perform the following tasks:

- Nullifies the steady-state error in frequency that is due to step load changes and thereby minimizes transient response and time error.
- Reduces the static change in tie-line power to zero due to step load retribution.
- Supplies the power to any area during emergency from the rest areas.

*Correspondence: 2018rsee008@nitjsr.ac.in

Department of Electrical Engineering, NIT Jamshedpur, Jamshedpur, Jharkhand 831014, India

A detailed review of LFC using PID controller based on soft computing, IMC techniques, and robust control schemes is presented in [2]. In [3], a PID controller with a sliding mode control scheme based on the ALO method for a four-area system is discussed, while a comparative analysis of a backtracking search algorithm and fruit fly optimizer-based PID controller for a two-area system considering nonlinearities is explained in [4]. Reference [5] uses a PID controller based on the ALO method for a two-area and a three-area system with a non-reheated thermal power system for analyzing different performance indices. In [6], a differential evolution (DE) method based on a PID controller is provided for a two-area thermal system with GRC and a two-area thermal system with diverse generating units such as thermal, hydro, and diesel. Reference [7] uses bacterial foraging optimization for LFC of an unequal three-area system, whereas a flower pollination algorithm-based PID controller is designed in [8] for frequency control of a two-area system considering GDB. A fuzzy PID controller based on a sine cosine algorithm for LFC of a hybrid renewable system is presented in [9], and [10] uses a sine cosine algorithm-based fuzzy PID controller for the LFC of a three-area system having nonlinearities. An imperialist competitive algorithm-based fuzzy PI controller for LFC of two-area systems is presented in [11], while [12] carries out a detailed review on the different types of fractional order controllers used for LFC where various controllers are used, including FOPI, FOPID, PIFOD, TID, FOPIDN, PFOID, etc. It has been observed from different literature surveys that FOPID is the most commonly used controller for LFC. The DE-based FOPID controller is used for LFC of a three-area system in [13], while a sine cosine algorithm-based TID controller is implemented for a two-area hybrid source system in [14]. FOPID based on gases Brownian motion optimization [15] is proposed for LFC of a two-area system having GDB, while a FOPID controller is designed in [16] for a single area system using Kharitonov's theorem. A Salp Swarm Algorithm (SSA) based TID controller is suggested in [17] for LFC for the systems incorporating FACTS devices, while a Grey wolf optimized multi-degree of freedom PID controller is proposed for the LFC of a two-area system in [18]. A 2-DOF-PID controller based on the quasi-oppositional Jaya algorithm is applied for LFC of multi-source three-area system in [19]. The 2-DOF-PID controller based on MFO is implemented for LFC of a two-area system [20], and it is also suggested for a two-area system with some nonlinearities in [21]. The SSA-based 2-DOF-PID controller is used in [22] for LFC of a two-area multi-source system. Some hybrid algorithms such as the hybrid gravitational search and pattern search algorithm [23], and the hybrid firefly-pattern search algorithm [24] have been proposed for LFC. Recently, ALO-based adaptive neuro fuzzy interference system (ANFIS) [25], PSO [26, 27], two-dimensional sine-logistic mapped-based SCA [28], and SSA [29, 30] have been used for LFC.

It is observed from the literature survey that in the study of LFC, the researchers have mainly focused on three things, viz. designing new controllers, proposing new optimization techniques, and modeling different types of power system. SCA is a recently developed technique that has been implemented to solve various engineering problems [31]. However, SCA suffers from slow convergence, and getting trapped in local optima. For better performance, SCA is improved in this work, and the Improved SCA (ISCA) method is applied to tune the controller of LFC. The 2-DOF-PID controller based on ISCA is designed and implemented for LFC of a three-area system with and without nonlinearities, and then further applied to a four-area system. The objective function used is ITAE, and by minimizing the ITAE, the different performance parameters such as peak undershoot, settling time of frequency and tie-line power are improved.

To further confirm the superiority of the proposed method, a statistical analysis is performed. For that analysis, each method is simulated for 20 independent runs, and the Wilcoxon Sign Rank Test (WSRT) is used. This is a significance test where $+, -, \approx$ show 'superior', 'inferior', or 'equivalent' with respect to the compared ones.

1.2 Contribution and organization of the paper

The main contributions of the work are as follows:

- An improved form of SCA is proposed, and the superiority of the proposed ISCA method is justified using unimodal and multimodal benchmark functions.
- The proposed ISCA is used to optimize the LFC controller variables, and then the performance is compared with some other recently developed algorithms such as SCA, ALO, SSA, and PSO.
- A three-area test system and a four-area test system are modeled for the case study.
- Three types of controllers, viz. PID, 2-DOF-PID, and FOPID are implemented to test the systems, and the effectiveness of the 2-DOF-PID controller is validated.
- For the first time, statistical analysis and WSRT are performed in LFC study to draw conclusions.
- The impact of the presence of physical constraints on system performance is investigated.

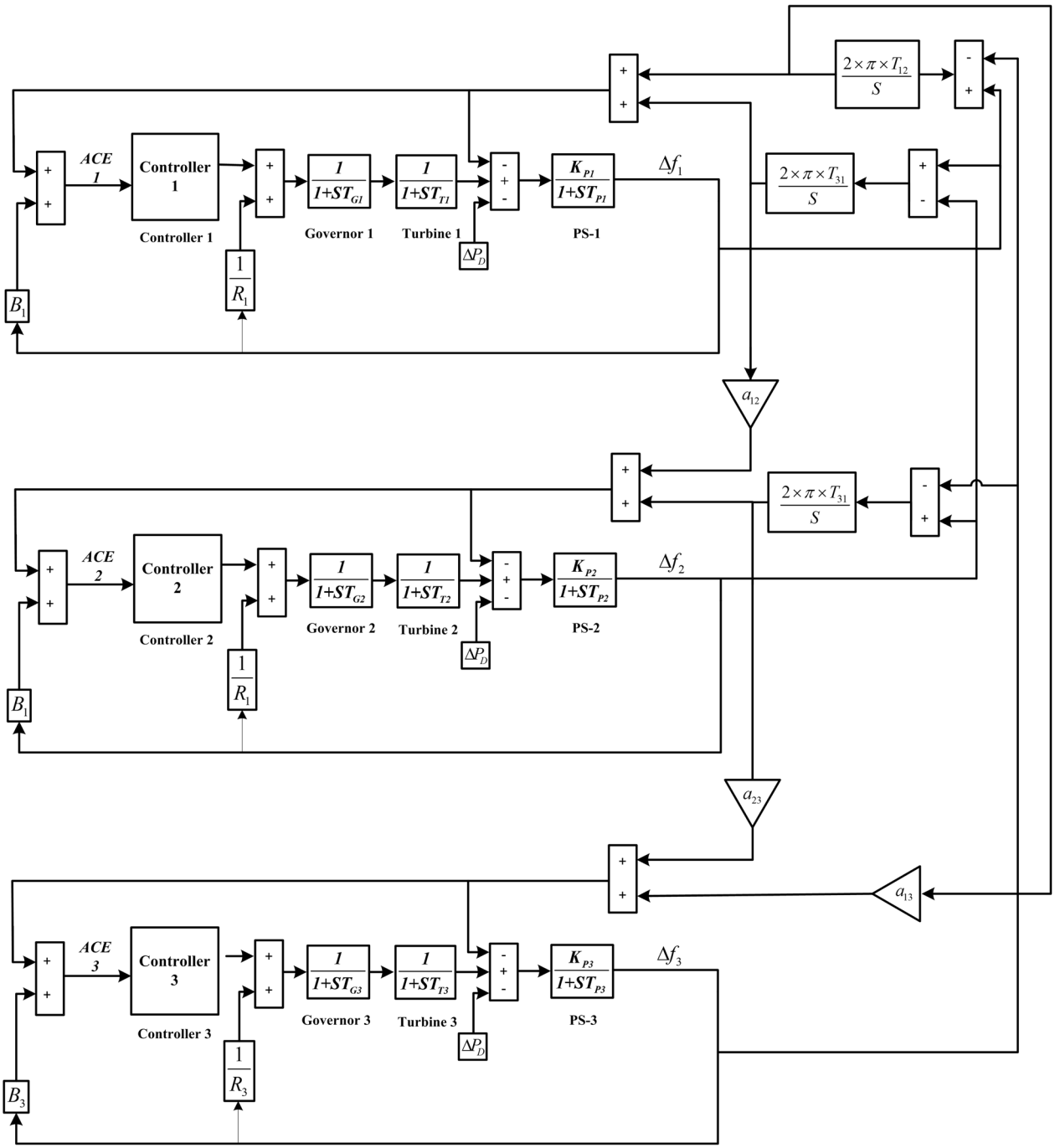

Fig. 1 Block diagram of a three-area power system

The work is organized as follows: the proposed power system is discussed in Sect. 2, while Sect. 3 describes the proposed controller. The proposed optimization strategy is detailed in Sect. 4, and the problem formulation is defined in Sect. 5. The results are discussed in Sect. 6, and the conclusions are summarized in Sect. 7.

2 Proposed power system

A three-area system is considered for the case study. The system is an unequal system that consists of three thermal generators having different parameter values. In each area, there are governor, turbine, generation and load sections. The complete system is shown in Fig. 1 with mathematical models in transfer function forms.

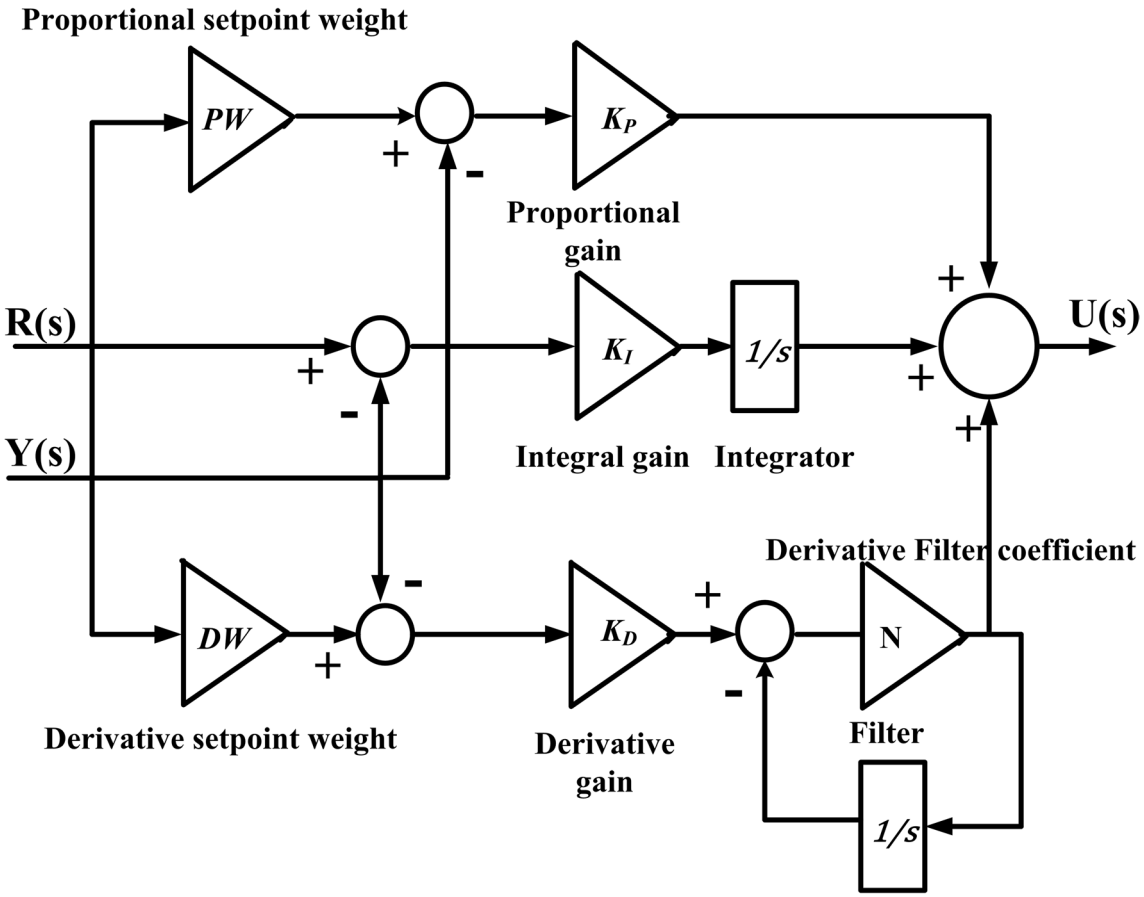

Fig. 2 Structure of the 2-DOF-PID controller

As shown in Fig. 1, the time constants of each area are denoted as: (1) T_{g1}, $T_{g2,}$ T_{g3} for the governors; (2) T_{t1}, T_{t2}, T_{t3} for the turbines; and (3) $T_{ps1,}$ T_{ps2}, T_{ps3} for the generation and load section. The gains for generation and load sections are denoted as K_{p1}, K_{p2}, K_{p3} for each area. The other parameters of the system are B_1, B_2, B_3 for the frequency biased, R_1, R_2, R_3 for the droops, and T_{12}, $T_{23,}$ T_{31} for the synchronizing coefficients. Drifts in frequency for each area are represented by ΔF_1, ΔF_2, ΔF_3, while $\Delta P_{tie}12$, ΔP_{tie23}, ΔP_{tie31} are the incremental changes in tie-line power. The numerical values of the parameters are shown in "Appendix 1".

3 The proposed controller

Numerous variants of PID controller have been used for many years, because of its simplicity and ability to provide reliable results. In this paper, a variation of PID controller known as 2-DOF- PID controller is used as the LFC controller because of its capability of fast disturbance rejection without significant increase of overshoot in set-point tracking. DOF stands for the degree of freedom, which means the extent of closed-loop transfer function that can be handled distinctly in a control system. The basic arrangement of this controller is shown in Fig. 2, where two separated loops can be seen. Two inputs are applied to the controller, of which one is a reference, and the other is the output of the system. The error signal generated because of difference in these two signals is used by the controller for the generation of the controller output signal which consists of the proportional, integral, and derivate portions according to their weight. The mathematical expression for the 2-DOF-PID is:

$$u = K_p\big((PW)r - y\big) + \frac{K_i}{s}\big(r - y\big) + \frac{K_d s}{Ns + 1}\big((DW)r - y\big) \tag{1}$$

where r and y are two input signals, r is a reference and y is the output of the system. K_p, K_i, K_d are the proportional, integral, and derivative weights, respectively. N is the filter coefficient, and u is the controller output. PW

and DW are the set-point weights on proportional and derivative sections, respectively.

4 The projected optimization techniques

4.1 Sine–cosine algorithm (SCA)

The SCA algorithm is a stochastic population-based optimization technique inspired by the mathematical functions of sine and cosine. It was recently developed in [32]. Because of the use of the sine and cosine mathematical functions, this algorithm provides cyclic space for exploitation, in which search agents can update their position as per a position changing equation, as:

$$Y_j^{n+1} = Y_j^n + a_1 \sin(a_2) \times \left| a_3 P_j^n - Y_j^n \right| \tag{2}$$

$$Y_j^{n+1} = Y_j^n + a_1 \cos(a_2) \times \left| a_3 P_j^n - Y_j^n \right| \tag{3}$$

where a_1, a_2, a_3 are the arbitrary numbers and are the main parameters of this algorithm, and Y_j^{n+1} and Y_j^n are the next and current positions of the solution at the time of the nth iteration in the jth dimension, respectively. P_j^n is the terminus point in the jth dimension. Equations (2) and (3) can be combined by another parameter a_4. Depending upon the value of a_4 which is an arbitrary numeral in the array of [0, 1], the algorithm will choose the equation for renovating the position of the investigating agent, given as:

$$Y_j^{n+1} = \begin{cases} Y_j^n + a_1 \sin(a_2) \times \left| a_3 P_j^n - Y_j^n \right| & if \quad a_4 < 0.5 \\ Y_j^n + a_1 \cos(a_2) \times \left| a_3 P_j^n - Y_j^n \right| & if \quad a_4 \geq 0.5 \end{cases} \tag{4}$$

The parameter a_1 will decide the next location province, which can be between the destination and another location. It has the objective of harmonizing the exploitation and exploration of this optimizer, and its value can be given by:

$$a_1 = b - n\frac{b}{N} \tag{5}$$

where N is the maximum number of iterations, b is a constant, and n represents the current iteration.The direction of movement of the search agent, whether towards the global optima or away from it, is decided by a_2. Better results are obtained by considering the range of a_2 between [−2 to 2], while sine and cosine functions are between 0 to 2π. The objective of a_3 is to emphasize the destination and is implemented by choosing a random value. If it is greater than 1 it will stochastically emphasize the destination while it will deemphasize if less than 1.

4.2 Improved sine–cosine algorithm (ISCA)

Nevertheless, SCA is very capable of handling the real-time problem, though there is scope to improve the algorithm to improve the rate of convergence, the ability not to be trapped in nearby optima, and to maintain a balance between exploration and exploitation. The above limitations of traditional SCA are due to the updating scheme of its search agents. In SCA, most of the search agents run towards the global optima, but sometimes can get trapped in local optima and thus converge to that premature local optima. To overcome this, a new scheme for updating the location of the search agent is introduced in this paper. This scheme mainly consists of the SCA/best-target shown in (6) and (7), and the SCA/rand-target shown in (8) and (9). The best-target search agent of the SCA assists the search agents in moving towards the best position obtained so far and searching locally around the best search agent, which results in the intensification of the solution. On the other hand, the rand-target search agent of SCA moves the search agents towards the arbitrary position, which results in more search space exploration. In the next step, the exploring capability of both schemes is combined by taking the mean as shown in (10), and the resultant is set as the new search agent. The characteristics of the proposed ISCA are as follows:

1. It maintains balance between exploration and exploitation.
2. It has fewer parameters, i.e., the number of parameters of the proposed ISCA is 3 while it is 4 in the original SCA.
3. It has a better convergence rate than the SCA.
4. It avoids getting trapped in local optima.

The values of the three parameters are decided in accordance with (11), (12), and (13), respectively.

$$Y_1 = Y_{best}^n + a_1 \sin(a_2) \times \left| a_3 Y_{rand}^n - Y_j^n \right| \tag{6}$$

$$Y_2 = Y_{best}^n + a_1 \cos(a_2) \times \left| a_3 Y_{rand}^n - Y_j^n \right| \tag{7}$$

$$Y_3 = Y_{rand}^n + a_1 \sin(a_2) \times \left| a_3 Y_{best}^n - Y_j^n \right| \tag{8}$$

$$Y_4 = Y_{rand}^n + a_1 \cos(a_2) \times \left| a_3 Y_{best}^n - Y_j^n \right| \tag{9}$$

$$Y_j^{n+1} = Mean(Y_1, Y_2, Y_3, Y_4) \tag{10}$$

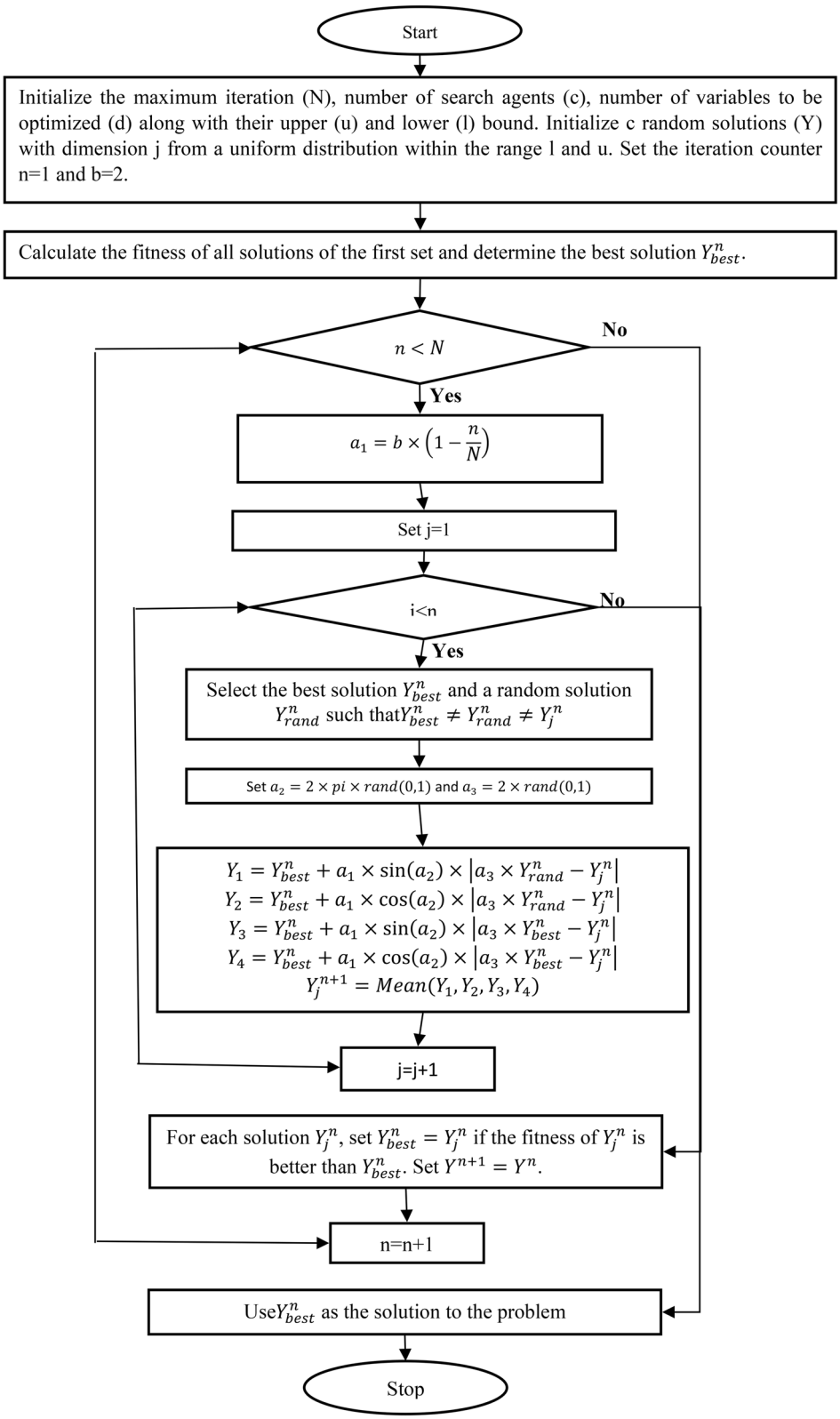

Fig. 3 Flow chart of ISCA

Table 1 Performance evaluation of ISCA over SCA, SSA, ALO, and PSO with the results of unimodal and multimodal benchmark test function

Function	ISCA		SCA		ALO		SSA		PSO	
	Mean	SD	Mean	SD	Mean	SD	Mean	SD	Mean	SD
F1	**9.861E−23**	1.9902E−22	5.09E−07	1.8181E−06	2.78E−08	5.51E−08	6.73E−05	2.78E−05	4.71E−19	1.95E−18
F2	**1.6083E−13**	2.55799E−13	5.92E−07	1.05E−06	8.52E−01	1.438721	1.67E−01	0.471005	1.4E−10	2.21E−10
F3	**1.8392E−11**	4.72532E−11	1.184673	2.160575127	4.31E−01	0.94951	4.81E−01	1.023026	0.002479	0.002992
F4	**1.2235E−07**	1.9916E−07	0.645629	2.739876	5.12E−03	0.006441	7.12E−03	0.00271	0.002384	0.003236
F5	**7.28815**	0.74182571	7.82433	0.488597	7.439	0.48539	7.8815	0.74182571	7.715811	10.01262
F6	1.02E−01	0.144505681	6.17E−01	0.239647	1.13E−08	6.74E−09	8.50E−05	2.96E−05	**9.82E−20**	2.35E−19
F7	**0.00166489**	0.001521864	0.004657	0.004711	5.42E−02	0.05512	5.24E−02	0.011685	0.003652	0.001909
F8	−2592.82	235.4926943	−2034.37	163.8136	− 2.32E+03	482.0453	− 2.72E+03	331.762	**− 3547.06**	234.6265
F9	2.180495	3.160774643	**1.706543**	4.872987	1.90E+01	9.676224	2.52E+01	8.30621	13.008369	6.522
F10	**2.9915E−13**	7.306E−13	1.4693E−6	4.5680E−6	5.00E−04	0.8121E−4	1.08E−2	0.7864E−01	6.78E−09	1.17E−9
F11	**0.0436073**	0.052779053	0.174077	0.173886	0.2324	0.27878	0.6492	0.714695	0.2326	0.27978
F12	0.02507793	0.01997888	0.148819	0.056735	2.73E+00	3.125277	7.05E−01	1.118442	**1.11E−19**	2.92E−19
F13	0.08798077	0.076773756	0.031108	0.099245	**2.15E−03**	0.00558	5.97E−03	0.00815	0.1137	0.1957

Bold value shows the best value

Table 2 Wilcoxon signed-rank test results on unimodal and multi-model functions indicating the inferior (-), superior (+), or equivalent (≈), method in comparison to the proposed method

Function	SCA	ALO	SSA	PSO
F1	−	−	−	−
F2	−	−	−	−
F3	−	−	−	−
F4	−	−	−	−
F5	≈	≈	≈	≈
F6	−	+	≈	+
F7	−	−	−	−
F8	≈	+	+	+
F9	+	−	−	−
F10	−	−	−	−
F11	−	−	−	−
F12	−	−	≈	+
F13	−	+	+	−

$$a_1 = b\left(1 - \frac{b}{N}\right) \tag{11}$$

$$a_2 = 2 \times \pi \times rand(0,1) \tag{12}$$

$$a_3 = 2 \times rand(0,1) \tag{13}$$

where b is a constant which is set to 2, N is the maximum number of iterations, n is the current iteration, and $rand(0,1)$ denotes a random number that will be generated in the range of 0–1.

The flow chart of the ISCA is shown in Fig. 3. The algorithm mainly has three steps, i.e., initialization, iteration, and termination. In the first step, the algorithm initializes the parameters, such as the maximum number of iterations (N), search agent number (c), number of variables to be tuned (d) with their upper (ub) and lower (lb) bound, first set of search agents (solution). In the second step, it generates a single new search agent by taking the average of four search agents which are being generated by the proposed search schemes. In the last step, the best agent so far obtained is selected as the solution to the optimization problem.

4.3 Performance estimation of the suggested method

The superiority of the proposed technique is tested against ALO, SCA, SSA, and PSO using the 13 standard unimodal and multimodal benchmark functions. Every single algorithm is run 20 times for each benchmark function. The average and standard deviations of different benchmark functions for the ISCA, SCA, ALO, SSA, and PSO algorithms are shown in Table 1. The statistical Wilcoxon signed-rank test is carried out on the results. This is shown in Table 2 to confirm the superiority of the ISCA. From Tables 1 and 2, it is found that the ISCA outperforms other methods in eight functions f_1,f_2,f_3,f_4,f_5,f_7,f_{10},f_{11}, while PSO outperforms other methods for f_6, f_8,f_{12} functions, and SCA and ALO outperform other methods for f_9 and f_{13} functions, respectively. Hence, the proposed method achieves better performance than the existing methods.

5 Problem formulation

Whenever there is a disturbance in the system, the prime objectives of LFC are: (1) nullifying the drift in frequency; and (2) keeping the exchange power of the tie-line at its schedule value. For any optimization problem in LFC, the objective function needs to be defined to achieve the objectives. Various criteria have been included in the literature to accumulate the frequency deviation and tie-line power deviation in the objective function. From the literature survey, it is found that ITAE (integral of time multiplied absolute error) is a promising criterion and is generally preferred over others like IAE, ISE, and ISTE. Hence, ITAE is used as the objective function for the test system shown in Fig. 1. In LFC, ITAE of the drift in each area frequency and incremental change in tie-line power is taken as the objective function:

$$J = ITAE = \sum_{i=1}^{NA} \int_{0}^{t_{sim}} \left(\left|\Delta f_i\right| + \sum_{\substack{j=1 \\ j \neq i}}^{NA} \left|\Delta P_{tie_{i-j}}\right| \right) .t.dt \tag{14}$$

where Δf_i is the drift in each area frequency, $\Delta P_{tie_{i-j}}$ is the incremental change in tie-line power, and t_{sim} is the simulation time period. The controller parameter boundary is the problem constraint. As a result, the design challenge can be expressed as an optimization problem:

Minimize J

For the PID controller

$$K_{p_{min}} \leq K_p \leq K_{p_{max}};\ K_{i_{min}} \leq K_i \leq K_{i_{max}};\ K_{d_{min}} \leq K_d \leq K_{d_{max}};\ N_{min} \leq N \leq N_{max},$$

For the FOPID controller:

$$K_{p_{min}} \leq K_p \leq K_{p_{max}};\ K_{i_{min}} \leq K_i \leq K_{i_{max}};\ K_{d_{min}} \leq K_d \leq K_{d_{max}};$$
$$\mu_{min} \leq \mu \leq \mu_{max};\ \lambda_{min} \leq \lambda \leq \lambda_{max}$$

For the 2-DOF-PID controller:

$$K_{p_{min}} \leq K_p \leq K_{p_{max}};\ K_{i_{min}} \leq K_i \leq K_{i_{max}};\ K_{d_{min}} \leq K_d \leq K_{d_{max}};$$
$$N_{min} \leq N \leq N_{max};\ b_{min} \leq b \leq b_{max};\ c_{min} \leq c \leq c_{max}$$

6 Results and discussions

On the test system of Fig. 1, many simulation studies have been carried out in order to determine the optimal combination of the suggested algorithm and the controller in order to reach a better outcome. For this purpose, various types of studies have been considered. In Sect. 6.1, the performance of various controllers is compared to identify the better one for further study, whereas in Sect. 6.2, disturbances are applied in two areas, while various algorithms are compared and statistical analysis is carried out. Similarly, in Sect. 6.3, disturbances are applied to all three areas, various algorithms are compared, and statistical investigation is carried out to find the better algorithm. In Sect. 6.4, nonlinearities of GRC, GDB, and commutation delay are considered in the test system, with various algorithms applied to find the controller parameters, while statistical analysis is carried out to find the better algorithm. For statistical assessment of these techniques, WSRT is performed to demonstrate the superior (+), equivalent (≈) or inferior (−) schemes in contrast to the proposed ISCA method. The study is then extended to a four-area power system shown in Fig. 8 in Sect. 6.5 and again various algorithms are compared for this scenario.

6.1 Examination of controllers

From the literature survey, it is found that some variants of PID controllers have been considered to implement the proposed algorithm. The most common controllers are the PID controller with filter (PIDF), 2-DOF-PID controller (2-DOF-PID), and Fractional order PID controller (FOPID). In this work, these controllers are initially compared for the considered test system (Fig. 1) to identify the better one for the present study. A disturbance of 2% is applied in area-1 and area-2. Figure 4 illustrates the convergence curve of the different controllers, the drift in frequency and tie-line power of each area for this case, while Table 3 shows the performance parameter of LFC for these controllers. From Table 3 and Fig. 4, it can be seen that the 2-DOF–PID controller outperforms the other two as it converges faster and attains the least objective function value. It also has a lower settling time and undershoot for the frequency deviation as well as for the tie-line power. Given these advantages of the 2-DOF-PID controller, it will be used as the LFC controller for further study as discussed in the following subsections.

6.2 Examination of optimization techniques when disturbances are in two areas

In this part, to validate the effectiveness of the proposed method, the ISCA is applied for the tuning of the LFC controller parameters. The 2-DOF-PID controlled test system is simulated when disturbances of 2% are applied in area-1 and area-2. The comparison is carried out with recently used algorithms of PSO, SSA, SCA, and ALO. Figure 5 illustrates the convergence curves and the transient responses of the test system. The convergence curves show that the ISCA achieves the lowest objective function (ITAE value) and converges faster than the

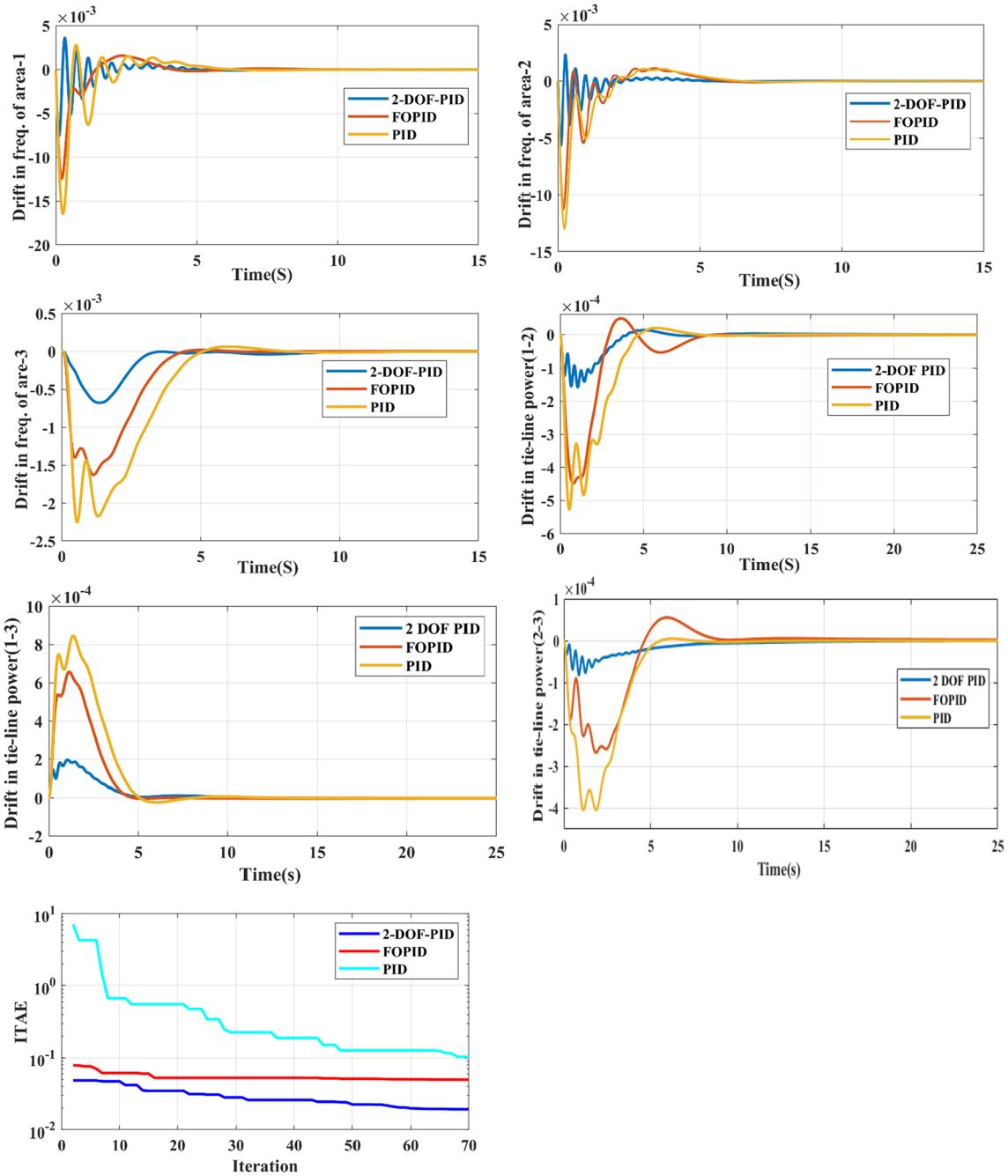

Fig. 4 Transient responses of frequency and tie-line power of all areas and convergence curves of the controllers for 2% SLD in area-1 and area-2 for 2-DOF PID, FOPIDF, and PID controllers

other methods. Table 4 gives the performance parameters of the different algorithms for this case. From Fig. 5 and Tables 4, it can be seen that the ISCA performs much better than the other optimization techniques.

To further highlight the efficacy of the ISCA in optimizing the LFC controller parameters, simulation is carried out for 20 independent times by ISCA, PSO, SSA, ALO, and SCA. Table 5 presents the mean and standard deviation of each technique. The ISCA gives the minimum mean value of the objective function. Further, for statistical assessment of these techniques, WSRT is performed on the test system for this scenario, and the results are shown in Table 5.

Table 3 Performance parameters of LFC with 2-DOF PID, FOPIDF, and PID controllers

Controller	ΔF_1	ΔF_2	ΔF_3	$\Delta P_{1-\Delta F_1 2}$	ΔP_{2-3}	ΔP_{3-1}
2-DOF PID						
Settling time	5.1195	5.6145	3.336	7.154	8.399	5.345
Maximum deviation	− 0.007548	-0.005649	-0.006749	-15.42×10^{-5}	-8.201×10^{-5}	-19.64×10^{-5}
FOPIDF						
Settling time	5.654	7.334	5.654	8.722	9.973	5.542
Maximum deviation	− 0.0124	0.01117	− 0.001626	-44.83×10^{-5}	-26.74×10^{-5}	-65.57×10^{-5}
PIDF						
Settling time	6.518	7.52	7.961	9.177	8.988	8.234
Maximum deviation	− 0.01643	− 0.013	− 0.002249	-52.69×10^{-5}	-4.036×10^{-5}	-84.69×10^{-5}

6.3 Examination of optimization techniques when the disturbance is in each area

In this section, the ISCA is used as the optimizer for the controller parameters. The 2-DOF-PID controlled test system is simulated when a disturbance of 2% is applied in each area of the test system, and the results are compared with the PSO, SSA, SCA, and ALO. Figure 6 compares the convergence curves and the transient responses of the test system. As seen, the convergence curve of the ISCA shows that the ISCA achieves the lowest objective function (ITAE value) and converges faster than the other methods. Table 6 gives the performance parameters of different algorithms for this case.

To further show the efficacy of the ISCA in optimizing the LFC controller parameters, simulation is done for 20 independent times by ISCA, PSO, SSA, ALO, and SCA. Table 7 presents the mean and standard deviation of each technique. The ISCA gives the minimum mean value of the objective function. Further, for statistical assessment of these techniques, WSRT is performed, and the results are given in Table 7. It is evident that the proposed method is superior.

6.4 Examination of optimization techniques considering physical constraints of GRC, GDB, and communication delay

In this section, the test system is modified and some physical constraints of GRC, GDB, communication delay, and reheated turbine are taken into consideration. Since practical power systems have nonlinearity as mentioned above, the modified system with consideration of these constraints gives a better representation of the practical systems. The communication delay of 40 ms, GDB of 0.036 pu, and GRC of 3% pu are considered in each area of the system, while a disturbance of 1% is applied to area-1. The proposed and other algorithms are compared for the 2-DOF-PID controlled system. The dynamic responses and convergence curves for this case are given in Fig. 7, and the performance parameters are shown in Table 8. It is concluded from the convergence curve, dynamic response, and performance parameters that the proposed ISCA method has much better tuning efficiency than other optimization methods.

To further highlight the efficacy of the ISCA in optimizing the LFC controller parameters, simulation is done for 20 independent times by ISCA, PSO, SSA, ALO, and SCA. Table 9 shows the mean and standard deviation of each technique. The ISCA gives the minimum mean value of the objective function. Further, for statistical assessment of these techniques, WSRT is performed and the results are given in Table 9.

6.5 Extension to four-area power system

To further examine the capability of the proposed algorithm the study is extended to a four-area power system. The schematic diagram of this system is shown in Fig. 8 while the values of relevant parameters are given in "Appendix 1". The 2-DOF-PID controlled system is simulated for the 2% disturbance in area-1. Figure 9 shows the comparative analysis with various techniques for this test system while Table 10 gives the corresponding performance parameters. From Fig. 9 and Table 10, it can be seen that the proposed ISCA algorithm performs better than other techniques.

To further demonstrate the efficacy of ISCA in optimizing the LFC controller parameters, simulation is done for 20 independent times by ISCA, PSO, SSA, ALO, and SCA. Table 11 shows the mean and standard deviation of each technique. The ISCA again gives the minimum mean value of the objective function. Again, WSRT is performed and the results are given in Table 11.

7 Conclusion

In this work, an improved version of the SCA, i.e. the ISCA, is proposed as the tuning tool for the load frequency controller of a multi-area unequal system. The balance between exploitation and exploration is

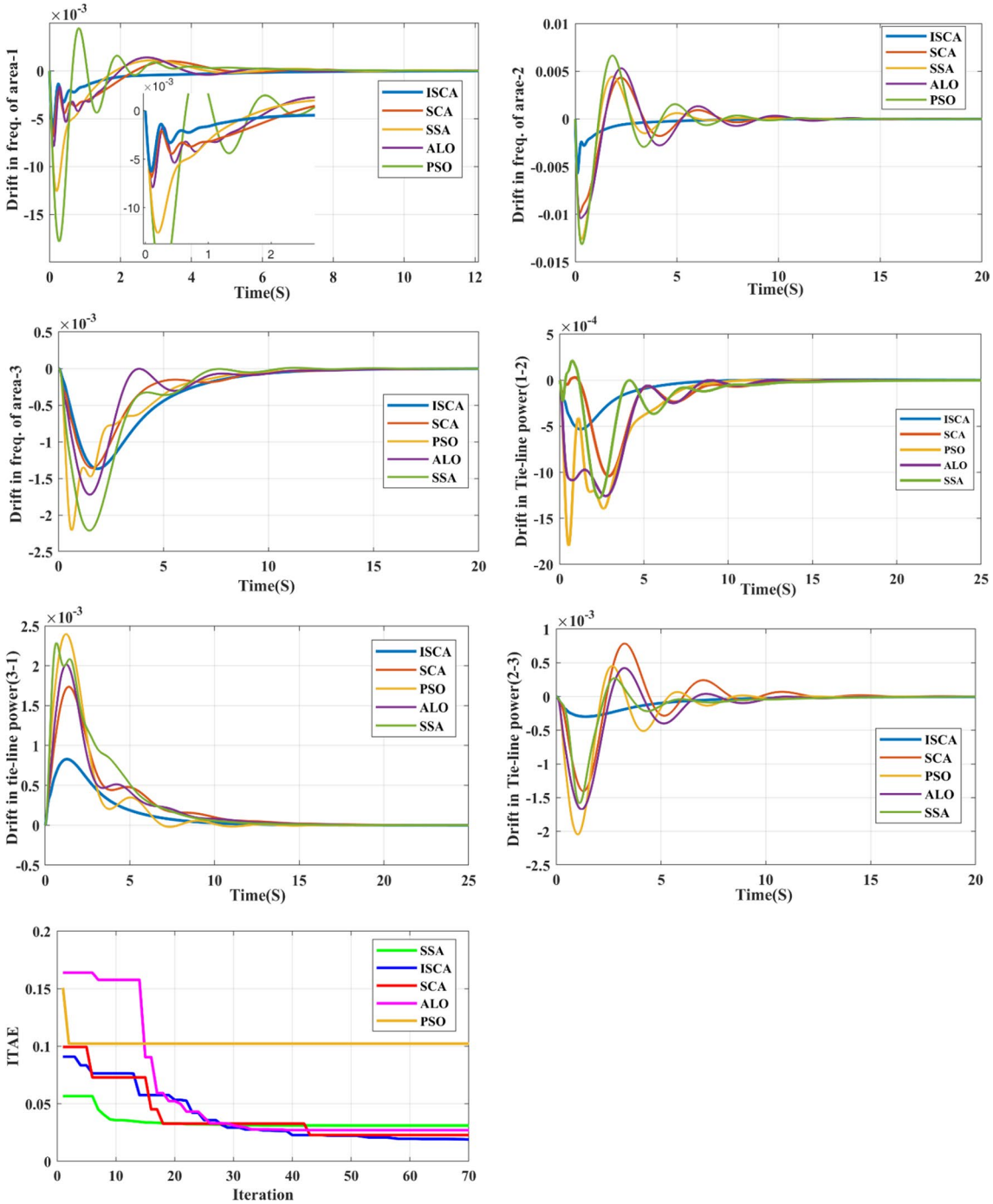

Fig. 5 Transient responses of frequency and tie-line power of all areas and convergence curves of the various algorithms for SLD of 2% in area-1 and area-2 with the proposed and other existing algorithms

maintained as the proposed method combines the exploitation proficiency of the SCA/best-target search agent and the exploration proficiency of the SCA/rand-target search agent. First, some controllers are compared for the considered test system, and the 2-DOF-PID controller emerges as the best. This is then

Table 4 Performance parameters of LFC with ISCA, SSA, ALO, SCA and PSO, in the case of SLD of 2% in area-1 and area-2

Algorithm	ΔF_1	ΔF_2	ΔF_3	ΔP_{1-2}	ΔP_{2-3}	ΔP_{3-1}
ISCA						
Settling time	9.1448	14.0824	15.083	21.615	12.7501	15.8758
Maximum deviation	− 0.00623	− 0.00561	− 0.00135	− 0.0005317	− 0.00029	0.000827
SCA						
Settling time	9.2762	16.243	17.671	22.612	19.1867	19.3867
Maximum deviation	− 0.06831	− 0.00984	− 0.00136	− 0.001047	− 0.00139	0.00173
ALO						
Settling time	9.2933	16.528	17.5261	22.703	17.6988	202,057
Maximum deviation	− 0.07899	− 0.01042	− 0.00172	− 0.001257	− 0.00167	0.002021
SSA						
Settling time	9.741	18.943	18.517	23.7924	19.4814	251.7936
Maximum deviation	− 0.01259	− 0.01262	− 0.00220	− 0.0017981	− 0.002047	0.002391
PSO						
Settling time	9.9342	19.224	19.3311	24.5246	19.802	22.7163
Maximum deviation	− 0.01748	− 0.01316	− 0.00221	− 0.001281	− 0.001581	0.002284

Table 5 Comparison of fitness values and WRST results of the three-area system with SLD of 2% in area-1 and area-2 using Different Optimization Techniques (Values in bold show best value)

	ISCA	SCA	ALO	SSA	PSO
Mean ± Std. Dev of Fitness Value	**0.0231175 ± 0.008800165**	0.031108 ± 0.012946	0.041118 ± 0.016742	0.068661 ± 0.018436	0.116889 ± 0.017588
Wilcoxon signed-rank test		–	–	–	–

Table 6 Performance parameters of LFC with ISCA, SSA, ALO, SCA and PSO in the case of SLD of 2% in each area

Algorithm	ΔF_1	ΔF_2	ΔF_3	ΔP_{1-2}	ΔP_{2-3}	ΔP_{3-1}
ISCA						
Settling time	10.7728	12.9398	13.0042	7.253	6.2267	10.965
Maximum deviation	− 0.00606	− 0.005649	− 0.00630	-5.744×10^{-5}	-1.9×10^{-5}	-1.972×10^{-5}
SCA						
Settling time	12.539	12.6376	14.288	16.717	13.6541	21.91
Maximum deviation	− 0.006370	− 0.01117	− 0.00630	-14.2×10^{-5}	-44.19×10^{-5}	-10.95×10^{-5}
ALO						
Settling time	19.1768	16.2105	15.315	17.4759	17.58	22.56
Maximum deviation	− 0.007476	− 0.009389	− 0.002249	-18.9×10^{-5}	-113.35×10^{-5}	-56.62×10^{-5}
SSA						
Settling time	15.2973	19.9389	19.6692	18.9614	16.5634	25.91
Maximum deviation	− 0.009796	− 0.008697	− 0.008903	49.62×10^{-5}	-73.22×10^{-5}	-44.47×10^{-5}
PSO						
Settling time	19.3201	19.8754	15.6837	20	20	29.759
Maximum deviation	− 0.013279	− 0.01183	− 0.01385	46.81×10^{-5}	-170.89×10^{-5}	-57.945×10^{-5}

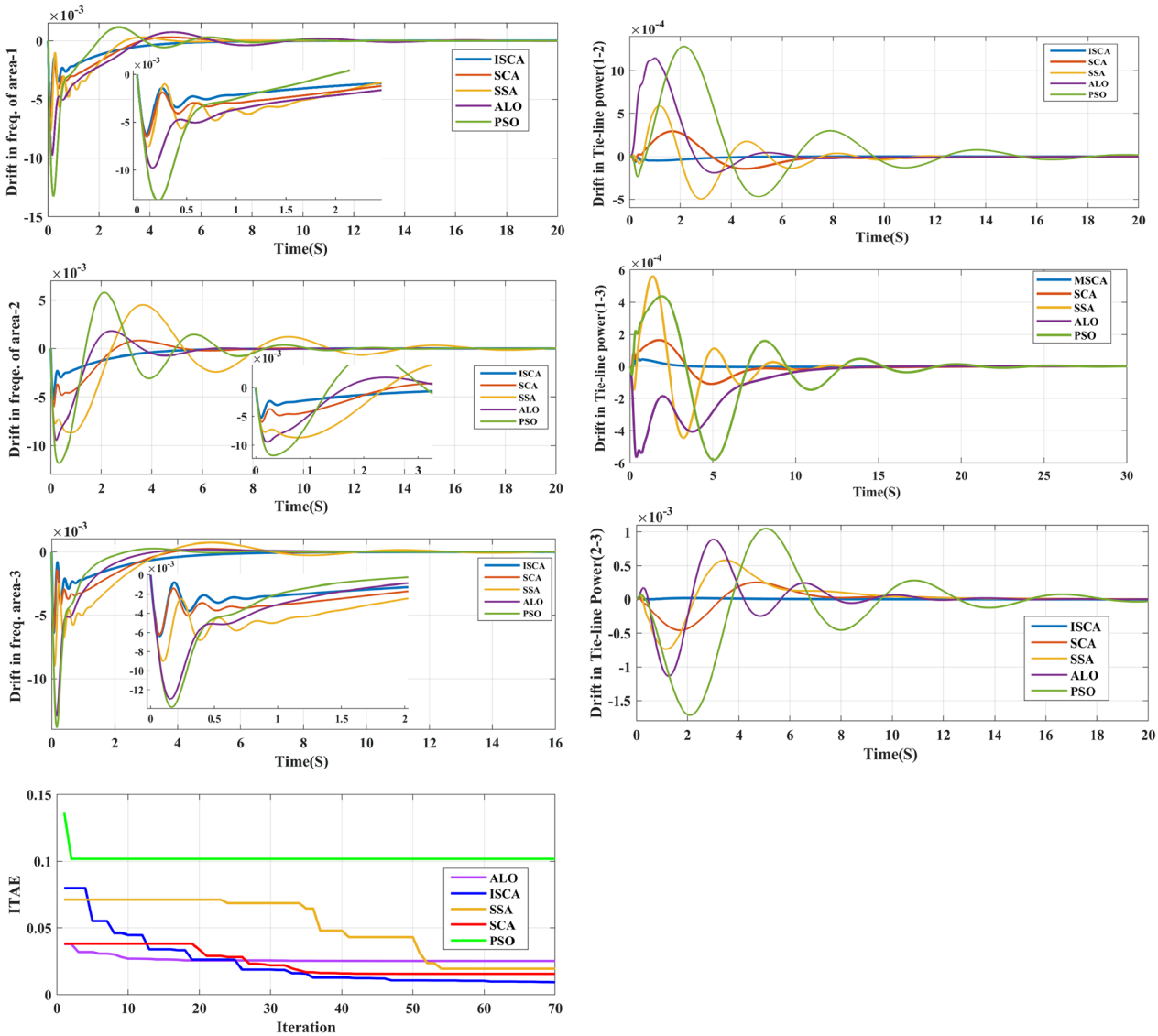

Fig. 6 Transient responses of frequency and tie-line power of all areas and convergence curves of the various algorithms for SLD of 2% in each area with the proposed and other algorithms

Table 7 Comparison of fitness values and WRST results of the three-area system with SLD of 2% in each area using Different Optimization Techniques (Values in bold shows best value)

	ISCA	SCA	ALO	SSA	PSO
Mean ± Std. Dev of Fitness Value	**0.01433026 ± 0.002703**	0.016443 ± 0.003433374	0.027976 ± 0.006409	0.021504 ± 0.00409	0.066433 ± 0.011953
Wilcoxon signed-rank test		–	–	–	–

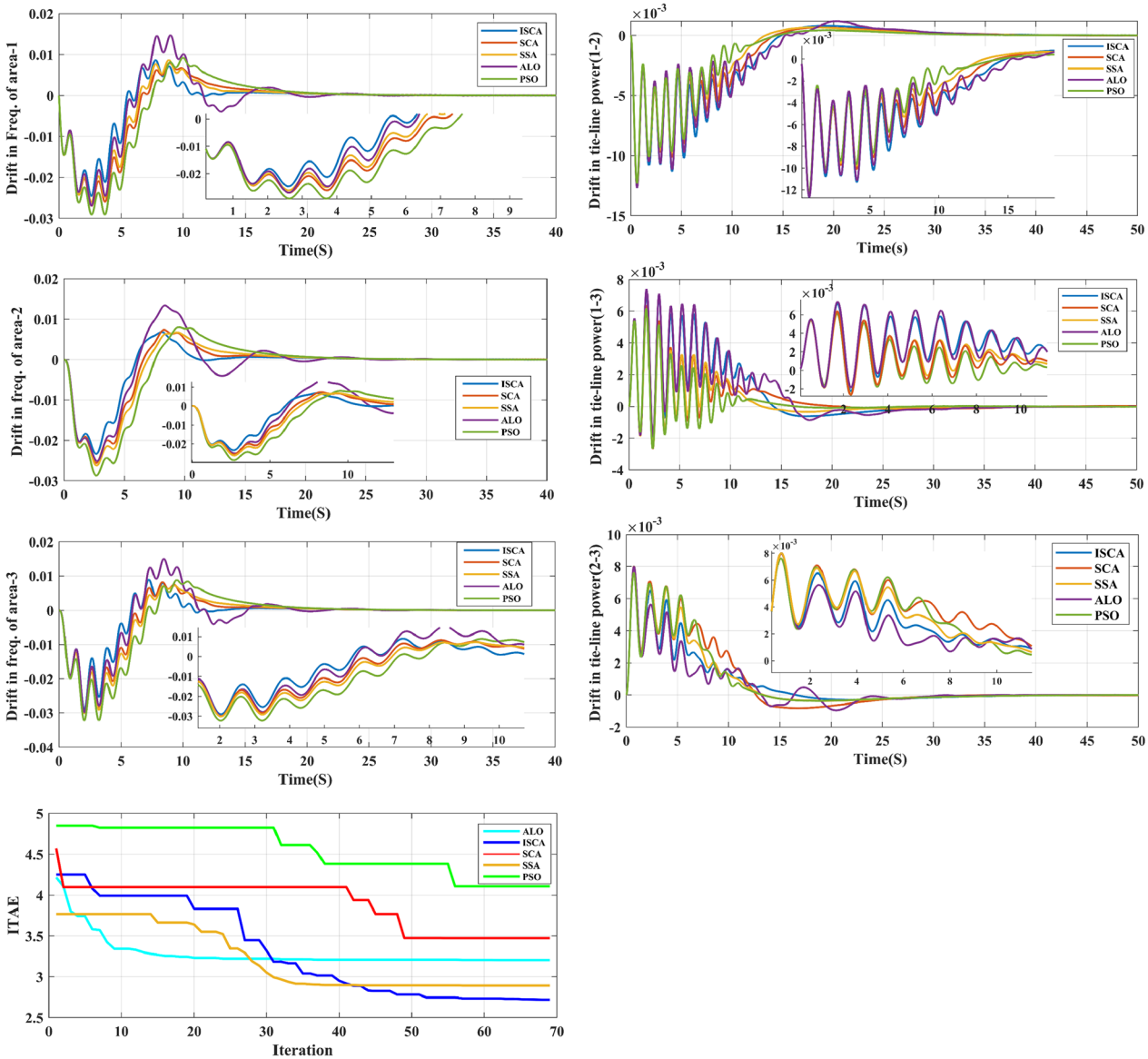

Fig. 7 Transient responses of frequency and tie-line power of all areas and convergence curves of the various algorithms for the three-area system with physical constraint and SLD of 1% in area-1 with the proposed and other algorithms

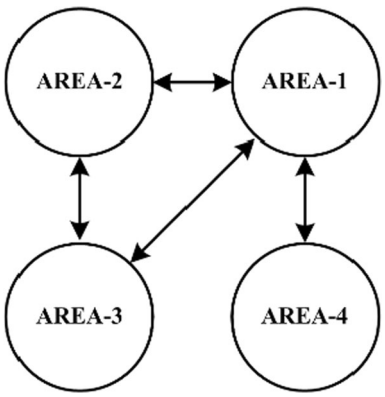

Fig. 8 Schematic diagram of the four-area system

further used as the load frequency controller for different analyses. The performance of the ISCA tuned LFC controller is examined for the test system for various schemes, such as disturbances in two areas, disturbance in each area, disturbance in the presence of various nonlinearities in the test system, and in an extended four-area power system. The performance of the ISCA is compared with some of the existing algorithms, while the effectiveness of the proposed method is tested by statistical analysis for different scenarios. After considering all the analyses, it is observed that the proposed method is better than the other techniques, such as PSO, SCA, SSA, and ALO, in terms of

Table 8 Performance parameters of LFC with ISCA, SCA, ALO, SSA, and PSO for the three-area system with physical constraints with SLD of 1% in area-1

Algorithm	ΔF_1	ΔF_2	ΔF_3	ΔP_{1-2}	ΔP_{2-3}	ΔP_{3-1}
ISCA						
Settling time	31.621	26.6702	28.5448	42.842	39.097	40.1447
Maximum deviation	− 0.02454	− 0.023358	− 0.029188	− 0.01268	− 0.00799	− 0.00229
SCA						
Settling time	32.5734	27.6502	29.062	43.354	48.7748	46.7889
Maximum deviation	− 0.026958	− 0.02543	− 0.02992	− 0.01287	0.00799	− 0.002646
ALO						
Settling time	39.784	35.3731	35.239	48.2348	47.7947	44.776
Maximum deviation	− 0.026958	− 0.024985	− 0.0301	− 0.01290	0.00800	− 0.00170
SSA						
Settling time	32.208	38.6619	38.269	49.212	45.4856	43.0036
Maximum deviation	− 0.026124	− 0.02618	− 0.030177	− 0.01259	0.00800	− 0.002651
PSO						
Settling time	36.3844	31.8903	34.141	43.6058	45.0462	47.3151
Maximum deviation	− 0.029081	− 0.028708	− 0.032206	− 0.01224	0.00755	− 0.002642

Table 9 Comparison of fitness values and WRST results of the three-area system with physical constraints with SLD of 1% in area-1 using Different Optimization Techniques (Values in bold shows best value)

	ISCA	**SCA**	**ALO**	**SSA**	**PSO**
Mean ± Std. Dev of Fitness Value	**2.76455 ± 0.030228369**	3.303025 ± 0.175311	3.043113 ± 0.226013	2.9268 ± 0.339249	4.0440 ± 0.639504
Wilcoxon signed-rank test results		–	–	–	–

Table 10 Performance parameters of LFC with ISCA, SSA, ALO, SCA and PSO in the case of SLD of 2% in area-1 of the four-area system

Algorithm	ΔF_1	ΔF_2	ΔF_3	ΔF_4	ΔP_{12}	ΔP_{13}	ΔP_{14}	ΔP_{23}
ISCA								
Settling time	2.970	17.849	15.691	12.691	22.791	14.912	16.803	20.652
Max. deviation	− 0.00669	− 0.00021	− 0.00058	− 0.00022	− 0.00121	0.00038	0.00044	0.00038
SCA								
Settling time	4.0291	20.9288	17.460	15.8243	16.5011	15.3838	17.5558	21.2028
Max. deviation	− 0.01177	− 0.00161	− 0.00081	− 0.00199	− 0.00339	0.00126	0.00118	0.00097
ALO								
Settling time	6.0434	22.342	16.762	19.234	15.501	15.420	17.6839	21.6339
Max. deviation	− 0.01522	− 0.00140	− 0.00099	− 0.00172	− 0.0.003	0.01275	0.00125	0.00101
SSA								
Settling time	6.0534	12.5877	16.893	15.8216	15.936	15.963	18.4623	22.017
Max. deviation	− 0.01013	− 0.00082	− 0.00238	− 0.00097	− 0.00232	0.00070	0.00089	0.00087
PSO								
Settling time	6.0644	8.9364	17.4604	154,219	14.691	16.721	19.3793	22.3421
Max. deviation	− 0.01702	− 0.00251	− 0.00052	− 0.00318	− 0.00444	0.00166	0.00155	0.00122

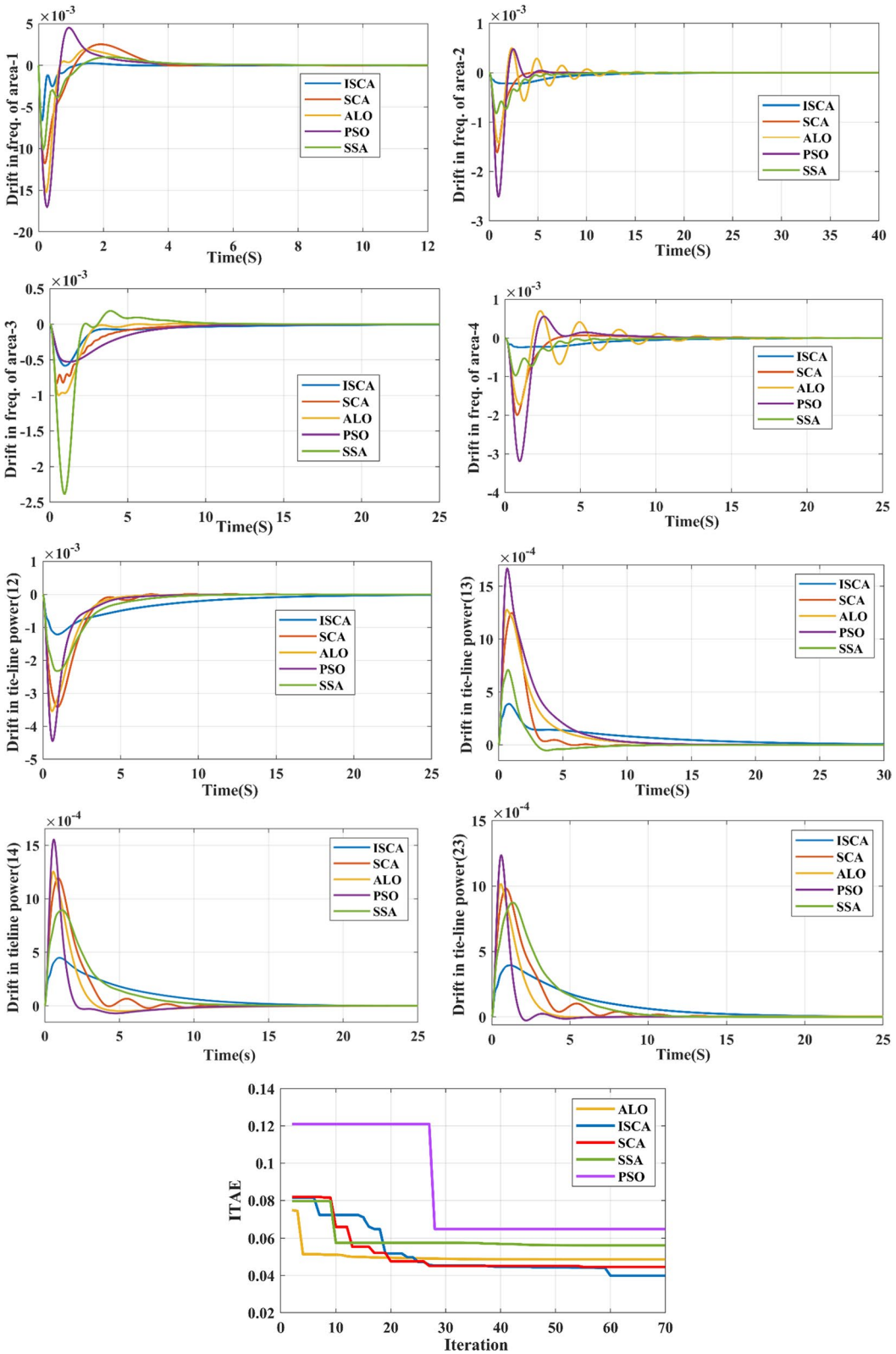

Fig. 9 Transient responses of frequency and tie-line power of all areas and convergence curves of the various algorithms for the four-area system with SLD of 2% in area-1 with the proposed and other algorithms

Table 11 Comparison of fitness values and WRST results of the four-area system with SLD of 2% in area-1 using Different Optimization Techniques (Values in bold shows best value)

	ISCA	SCA	ALO	SSA	PSO
Mean ± Std. Dev of Fitness Value	**0.03988 ± 0.008800165**	0.0446 ± 0.012946	0.04843 ± 0.01672	0.056202 ± 0.018436	0.0649 ± 0.017588
Wilcoxon signed-rank test results		–	–	–	–

better convergence rate, least objective function value, minimum settling time, and undershoot of deviation in frequency and tie line power. Therefore, it can be concluded that the proposed method can be applied to solve real-world engineering problems.

Appendix 1

Three area unequal power system

$T_{g1} = 0.08$; $T_{g2} = 0.06$; $T_{g3} = 0.07$; $T_{t1} = 0.4$ $T_{t2} = 0.44$; $T_{t3} = 0.3$; $K_{p1} = 105$; $K_{p2} = 100$; $K_{p3} = 120$; $T_{ps1} = 20$; $T_{PS2} = 22$; $T_{ps3} = 20$; $B_1 = 0.3483$; $B_2 = 0.3827$; $B_3 = 0.3692$; $R_1 = 3$; $R_2 = 2.73$; $R_3 = 2.82$; $T_{12} = 0.2$ $T_{23} = 0.44$ $T_{31} = 0.3$.

Four area unequal power system

$T_{g1} = 0.08$; $T_{g2} = 0.06$; $T_{g3} = 0.07$, $T_{g4} = 0.06$; $T_{t1} = 0.4$ $T_{t2} = 0.44$; $T_{t3} = 0.3$, $T_{t4} = 0.44$; $K_{p1} = 105$; $K_{p2} = 100$; $K_{p3} = 120$, $K_{p4} = 100$; $T_{ps1} = 20$; $T_{ps2} = 22$; $T_{ps3} = 20$; $T_{ps1} = 22$; $B_1 = 0.3483$; $B_2 = 0.3827$; $B_3 = 0.3692$; $B_4 = 0.3827$; $R_1 = 3$; $R_2 = 2.73$; $R_3 = 2.82$; $R_4 = 2.73$; $T_{12} = 0.2$ $T_{23} = 0.44$ $T_{31} = 0.3$; $T_{14} = 0.2$.

Abbreviations

ISCA: Improved sine–cosine algorithm; ALO: Ant-lion optimization; LFC: Load frequency control; DOF: Degree of freedom; T_{ps}: Time constant of the power system; FOPID: Fractional order proportional-integral-derivative; SCA: Sine–cosine algorithm; T_{sg}: Time constant of speed governor; R_i: Speed regulation constant; K_{ps}: Gain of the power system; PID: Proportional-integral-derivative; β: Frequency bias constant; SSA: Salp swarm algorithm; PW, DW: Proportional and derivative set-point weights respectively; T_t: Time constant of the turbine; ΔP_{tie}: Tie-line power deviation; T_{ij}: Synchronization time constant; ΔP_{ref}: Reference input to the controller; PSO: Particle swarm optimization; ΔP_D: Load disturbance; Δf: Frequency deviation; WRST: Wilcoxon sign rank test; SLD: Step load disturbance; GRC: Generation Rate Constraint; GDB: Governor dead band.

Acknowledgements

Not applicable.

Author contributions

NKG: Formulation of the method, Simulation and Result, Paper writing. MKK: Formulation of the method. AKS: Supervisions and Paper correction. All authors read and approved the final manuscript.

Authors' information

Neelesh Kumar Gupta born in 1991. He received B. Tech degree form UPTU Lucknow, Utter Pradesh, India in electrical and electronics engineering in 2014, M. Tech in Power System Engineering from NIT Jamshedpur, Jharkhand, India, in 2018. Currently he is the Research Scholar in Electrical Engineering department of NIT Jamshedpur Jharkhand, India.

Manoj Kumar Kar born in 1988. He received B. Tech degree from B.P.U.T, Odisha India, in 2010, M. Tech (Power Electronics and Control Drives) from VSSUT, Burla, Odisha, India, in 2012. He is having five years of teaching experience. Currently, he is the Research Scholar in the Electrical Engineering Department, NIT Jamshedpur Jharkhand, India.

Arun Kumar Singh born in 1956. He received his B. Sc. (Engg.) degree from Kurkshetra University, India in 1982, M Tech from IIT BHU, India in 1985, Ph.D. from IIT Kharagpr, India in 1994. He is having more than thirty years of teaching experience. Currently, he is working as Professor in the Electrical Engineering Department, NIT Jamshedpur Jharkhand, India.

Funding

No funding has been received for this work.

Availability of data and materials

The datasets used and/or analysed during the current study are available from the corresponding author on reasonable request.

Declarations

Competing interests

The authors declare that they have no known competing financial interests or personal relationships that could have appeared to influence the work reported in this paper.

Received: 11 March 2022 Accepted: 4 August 2022
Published online: 01 September 2022

References

1. Kundur, P. (2009). *Power system stability and control* (8th ed.). Tata McGraw-Hill.
2. Hote, Y. V., & Jain, S. (2018). PID controller design for load frequency control: Past, present and future challenges. *IFAC-PapersOnLine, 51*(4), 604–609. https://doi.org/10.1016/j.ifacol.2018.06.162
3. Ah, G. H., & Li, Y. Y. (2020). Ant lion optimized hybrid intelligent PID-based sliding mode controller for frequency regulation of interconnected multi-area power systems. *Transactions of the Institute of Measurement and Control, 42*(9), 1594–1617. https://doi.org/10.1177/0142331219892728
4. Dinesh Madasu, S., Sai Kumar, M. L. S., & Singh, A. K. (2017). Comparable investigation of backtracking search algorithm in automatic generation control for two area reheat interconnected thermal power system. *Applied Soft Computing, 55*, 197–210. https://doi.org/10.1016/j.asoc.2017.01.018
5. Jagatheesan, K., Anand, B., Dey, K. N., Ashour, A. S., & Satapathy, S. C. (2018). Performance evaluation of objective functions in automatic generation control of thermal power system using ant colony optimization technique-designed proportional–integral–derivative controller. *Electrical Engineering, 100*(2), 895–911. https://doi.org/10.1007/S00202-017-0555-X
6. Mohanty, B., Panda, S., & Hota, P. K. (2014). Differential evolution algorithm based automatic generation control for interconnected power systems with non-linearity. *Alexandria Engineering Journal, 53*(3), 537–552. https://doi.org/10.1016/j.aej.2014.06.006
7. Nanda, J., Mishra, S., & Saikia, L. C. (2009). Maiden application of bacterial foraging-based optimization technique in multiarea automatic

generation control. *IEEE Transactions on Power Systems, 24*(2), 602–609. https://doi.org/10.1109/TPWRS.2009.2016588
8. Madasu, S. D., Sai Kumar, M. L. S., & Singh, A. K. (2018). A flower pollination algorithm based automatic generation control of interconnected power system. *Ain Shams Engineering Journal*. Retrieved June 05, 2021, from https://reader.elsevier.com/reader/sd/pii/S2090447916300892?token=888DDE26161EBD8536B32321A023F501D4402644778263B171C2669901F5B191A3543FB2C83D59DD636863E6AEAA35DF&originRegion=eu-west-1&originCreation=20210605180519
9. Rajesh, K. S., & Dash, S. S. (2019). Load frequency control of autonomous power system using adaptive fuzzy based PID controller optimized on improved sine cosine algorithm. *Journal of Ambient Intelligence and Humanized Computing, 10*(6), 2361–2373. https://doi.org/10.1007/s12652-018-0834-z
10. Sahu, P. C., Prusty, R. C., & Sahoo, B. K. (2020). Modified sine cosine algorithm-based fuzzy-aided PID controller for automatic generation control of multiarea power systems. *Soft Computing, 24*(17), 12919–12936. https://doi.org/10.1007/s00500-020-04716-y
11. Arya, Y. (2018). Automatic generation control of two-area electrical power systems via optimal fuzzy classical controller. *Journal of the Franklin Institute, 355*(5), 2662–2688. https://doi.org/10.1016/j.jfranklin.2018.02.004
12. Latif, A., Hussain, S. M. S., Das, D. C., Ustun, T. S., & Iqbal, A. (2021). A review on fractional order (FO) controllers' optimization for load frequency stabilization in power networks. *Energy Reports, 7*, 4009–4021. https://doi.org/10.1016/J.EGYR.2021.06.088
13. Delassi, A., Arif, S., & Mokrani, L. (2018). Load frequency control problem in interconnected power systems using robust fractional PIλD controller. *Ain Shams Engineering Journal, 9*(1), 77–88. https://doi.org/10.1016/j.asej.2015.10.004
14. Khadanga, R. K., Kumar, A., & Panda, S. (2021). A novel sine augmented scaled sine cosine algorithm for frequency control issues of a hybrid distributed two-area power system. *Neural Computing and Applications*. https://doi.org/10.1007/s00521-021-05923-w
15. Zamani, A., Barakati, S. M., & Yousofi-Darmian, S. (2016). Design of a fractional order PID controller using GBMO algorithm for load–frequency control with governor saturation consideration. *ISA Transactions, 64*, 56–66. https://doi.org/10.1016/j.isatra.2016.04.021
16. Sondhi, S., & Hote, Y. V. (2016). Fractional order PID controller for perturbed load frequency control using Kharitonov's theorem. *International Journal of Electrical Power & Energy Systems, 78*, 884–896. https://doi.org/10.1016/j.ijepes.2015.11.103
17. Sharma, M., Prakash, S., Saxena, S., & Dhundhara, S. (2021). Optimal fractional-order tilted-integral-derivative controller for frequency stabilization in hybrid power system using salp swarm algorithm. *Electrical Power Components and Systems, 48*(18), 1912–1931. https://doi.org/10.1080/15325008.2021.1906792
18. Charan Patel, N., Kumar Debnath, M., Prasad Bagarty, D., & Das, P. (2018). GWO tuned multi degree of freedom PID controller for load frequency control. *International Journal of Engineering & Technology, 7*(3.3), 548. https://doi.org/10.14419/ijet.v7i2.33.14831
19. Guha, D., Roy, P. K., & Banerjee, S. (2020). Quasi-oppositional JAYA optimized 2-degree-of-freedom PID controller for load-frequency control of interconnected power systems. *International Journal of Modelling and Simulation, 00*(00), 1–23. https://doi.org/10.1080/02286203.2020.1829444
20. Singh, R., Kesarwani, S. K., Gupta, N. K., & Ashfaq, H. (2020). Design of 2-Dof Pid controller for load frequency control of two area power system using Mfo algorithm. *International Journal of Engineering and Advanced Technology, 9*(3), 158–161. https://doi.org/10.35940/ijeat.c5009.029320
21. Sahu, R. K., Panda, S., & Rout, U. K. (2013). DE optimized parallel 2-DOF PID controller for load frequency control of power system with governor dead-band nonlinearity. *International Journal of Electrical Power & Energy Systems, 49*(1), 19–33. https://doi.org/10.1016/j.ijepes.2012.12.009
22. Mohapatra, T. K., Dey, A. K., & Sahu, B. K. (2020). Employment of quasi oppositional SSA-based two-degree-of-freedom fractional order PID controller for AGC of assorted source of generations. *IET Generation, Transmission and Distribution, 14*(17), 3365–3376. https://doi.org/10.1049/iet-gtd.2019.0284
23. Sahu, R. K., Panda, S., & Padhan, S. (2015). A novel hybrid gravitational search and pattern search algorithm for load frequency control of nonlinear power system. *Applied Soft Computing Journal, 29*, 310–327. https://doi.org/10.1016/j.asoc.2015.01.020
24. Sahu, R. K., Panda, S., & Pradhan, P. C. (2015). Design and analysis of hybrid firefly algorithm-pattern search based fuzzy PID controller for LFC of multi area power systems. *International Journal of Electrical Power & Energy Systems, 69*, 200–212. https://doi.org/10.1016/j.ijepes.2015.01.019
25. Fathy, A., & Kassem, A. M. (2019). Antlion optimizer-ANFIS load frequency control for multi-interconnected plants comprising photovoltaic and wind turbine. *ISA Transactions, 87*, 282–296. https://doi.org/10.1016/j.isatra.2018.11.035
26. Pain, S., & Acharjee, P. (2014). Multiobjective optimization of load frequency control using PSO. *International Journal of Emerging Technology and Advanced Engineering, 4*(7), 16–22.
27. Jaber, A. S., Ahmad, A. Z., & Abdalla, A. N. (2013). An investigation of scaled-FLC using PSO for multi-area power system load frequency control. *Energy and Power Engineering, 05*(04), 458–462. https://doi.org/10.4236/epe.2013.54b088
28. Khokhar, B., Dahiya, S., & Parmar, K. P. S. (2021). Load frequency control of a microgrid employing a 2D sine logistic map based chaotic sine cosine algorithm. *Applied Soft Computing, 109*, 107564. https://doi.org/10.1016/j.asoc.2021.107564
29. Sharma, M., Prakash, S., & Saxena, S. (2021). Robust load frequency control using fractional-order TID-PD approach via salp swarm algorithm. *IETE Journal of Research*. https://doi.org/10.1080/03772063.2021.1905084
30. Khokhar, B., Dahiya, S., & Singh-Parmar, K. P. (2020). A robust cascade controller for load frequency control of a standalone microgrid incorporating electric vehicles. *Electric Power Components and Systems, 48*(6–7), 711–726. https://doi.org/10.1080/15325008.2020.1797936
31. Mirjalili, S. M., Mirjalili, S. Z., Saremi, S., & Mirjalili, S. (2020). *Sine cosine algorithm: Theory, literature review, and application in designing bend photonic crystal waveguides* (Vol. 811). Springer.
32. Mirjalili, S. (2016). SCA: A sine cosine algorithm for solving optimization problems. *Knowledge-Based Systems, 96*, 120–133. https://doi.org/10.1016/j.knosys.2015.12.022